Title

Structure and water dynamics of aqueous peptide solutions in the presence of co-solvents

Journal

Physical Chemistry Chemical Physics, 12(2)

ISSN

0956-5000

Authors

Malardier-Jugroot, Cecile
Bowron, Daniel T
Soper, Alan K
et al.

Publication Date

2010-01-14

DOI

10.1039/b915346b

Peer reviewed

Structure and Water Dynamics of Aqueous Peptide Solutions in the Presence of Co-Solvents

Cecile Malardier-Jugroot
Department of Chemistry and Chemical Engineering, Royal Military College of Canada, Kingston, K7K 7B4, Canada

Daniel T. Bowron and Alan K. Soper
ISIS Facility, STFC Rutherford Appleton Laboratory, Harwell Science and Innovation Campus, Didcot, Oxon, OX11 0QX, United Kingdom

Margaret E. Johnson[1,2,3] and Teresa Head-Gordon[1,2,3*]
[1]*UCSF/UCB Joint Graduate Group in Bioengineering*
[2]*Department of Bioengineering, University of California, Berkeley*
[3]*Physical Biosciences Division, Lawrence Berkeley National Laboratory*
Berkeley, California 94720 USA

We perform neutron diffraction and quasi-elastic neutron scattering (QENS) to probe hydration water structure, and dynamics down to supercooled temperatures, of a concentrated amphiphilic peptide system with the co-solvents glycerol and dimethyl sulfoxide. We find that the kosmotropic co-solvent glycerol preserves the hydration structure near the peptide that is observed in the water solvent alone, that in turn preserves the dynamical temperature trends of two water relaxation processes- one corresponding to a localized relaxation process of the peptide bound surface water and a second relaxation process of the outer hydration layers. By contrast the chaotropic co-solvent, by disrupting the hydration layer near the peptide surface, eliminates the inner hydration layer relaxation process induced by the peptide, to show a single timescale for translational water dynamics.

*To whom correspondence should be addressed.

INTRODUCTION

The formulation of effective co-solvents is important in biopharmaceutical production of peptide and proteins to improve their long-term storage and delivery[1]. Non-aqueous solvents such as trifluoro-ethanol or methanol can lead to specific stabilization of certain secondary structural motifs[2], and co-solvents such as glycerol or trehalose are stabilizers that have cryoprotective properties for proteins[3,4]. Protein folding reactions and experimental models of the random coil state typically use denaturants such as guanidine hydrochloride, urea, or dimethyl sulfoxide (DMSO) to destabilize the native state[5,6], although DMSO can also act as a protein stabilizer at certain concentrations[7]. These results suggest that understanding solvent environmental influences may lead to the ability to exploit not only differences in monomer composition but solvent composition, to create biological and non-biological polymers with desired properties.

Empirical evidence has accumulated that denaturants and non-denaturants interact differently with the water co-solvent and protein solute that influences protein stability, self-assembly, and activity properties[8, 9]. Chaotropes (protein destabilizers) are thought to be "pushed" onto the protein surface, thereby depleting the hydration layer and decreasing water's surface tension to promote denaturation by now favored exposure of hydrophobic groups[10]. By contrast, kosmotropes (protein stabilizers) are instead excluded from the protein surface due to their enhanced solubility in the water phase, which increases the surface tension of water to oppose the exposure of hydrophobic groups to stabilize the folded state[10]. However, it is also observed that the same co-solvent can serve as either a stabilizing or destabilizing agent under varied conditions that may depend on the protein, on the water content, on temperature, on co-solvent concentration, or some combination of all variables[7,11,12]. Presently we don't know whether co-solvents promote (or decrease) protein stabilization through selective hydration of certain amino acid side chains, or how specific water and co-solvent interactions might change as a function of temperature. Exceptions to the "rules" for chaotrope vs. kosmotrope solvation based on these simple thermodynamic or structural arguments do not allow for the possibility that the kinetics may be important, and relative timescales of motion of the constituents of co-solvent protein solutions are much more poorly characterized and understood than structure.

The complexity of protein systems has led to consideration of simplified representations that might serve as reduced models of a protein's hydration. Our group has focused on understanding hydration environment through the study of individual blocked amino acids as a function of their

concentration in water.[13-20] The role of hydration in the earlier steps of folding are mimicked when the local concentration of amino acids is relatively dilute, while more concentrated solutions describe the consequences of hydration of the folded protein surface when solvent shells overlap. This can be viewed as a model systems approach for the characterization of hydration or environmental influence on protein self-assembly or co-assembly, invoking an approximation that collapsed polymers can be modeled by increasing the effective local concentration of monomers.

In this paper we perform neutron diffraction and quasi-elastic neutron scattering (QENS) at two resolutions that probe timescales of picoseconds to nanoseconds on a concentrated peptide system, N-acetyl-leucine-methylamide (NALMA, Figure 1), in aqueous solution with co-solvents glycerol (non-ionic kosmotrope) and DMSO (non-ionic chaotrope). We have previously reported QENS experiments for the water dynamics in a concentrated solution of NALMA without co-solvents over a temperature range of 248K to 288K, in which we observed two translational components when analyzed under a combination of the jump diffusion model and the relaxation cage model.[17] We determined that the first translational motion is a localized relaxation process of the bound surface water, while the second relaxation process is a dynamical signature of more fluid water that exhibited a non-Arrhenius dependence on temperature.

Here we contrast the structure and dynamics of the original peptide system when co-solvents are added and characterized over a similar temperature range. We find that the kosmotropic glycerol co-solvent preserves all of the qualitative structural features of hydration water and the dynamical temperature dependence of the two water relaxation processes, while the DMSO co-solvent, by displacing the hydration layer from the peptide surface altogether, thereby eliminates the dynamical component arising from the solute hydration layer.

EXPERIMENTAL METHODS

Solution Preparations

We prepared peptide, water, and co-solvent solutions in molar quantities designed to keep the ratio of solutes molecules to solvent molecules (H_2O + co-solvent) equivalent to our previous 1M NALMA aqueous solution studies. In particular, co-solvent mixtures studied included: (1) deuterated NALMA, deuterated d8-glycerol and H_2O in a molar ratio of 1:1:5 and (2) deuterated NALMA, deuterated DMSO, and H_2O in a molar ratio of 1:1:4. For the liquid diffraction experiments, we sometimes replaced H_2O with D_2O or HDO for these solutions depending on

experiment (see below). We also prepared water and co-solvent solutions of (1) d8-glycerol and H_2O in a molar ratio of 1:5 and (2) d-DMSO and H_2O in a molar ratio of 1:4. Each solution was sonicated for 15 min and centrifuged for 10 min at 10,000g. All deuterated materials were purchased from CDN Isotopes[21].

Neutron diffraction experiments

The neutron liquid diffraction data were collected using the small angle neutron diffractometer for amorphous and liquid sample (SANDALS) at the ISIS pulsed neutron source at the Rutherford Appleton Laboratory, Oxfordshire, U.K. Each sample was contained in a container made of a Ti0.68Zr0.32 alloy; this alloy composition gives no coherent neutron scattering contribution to the measured signal of the cell. The sample container is a flat plate of internal dimensions 1 mm × 35 mm × 35 mm with a wall thickness of 1.1 mm. The scattering data were collected and analyzed using neutrons wavelengths in the range λ = 0.075−3.5 Å over a corresponding Q-range for each data set of 0.1−30$Å^{-1}$. After collection, the data were analyzed using the program Gudrun, available at ISIS[22] to correct the data for the contributions from the empty cell, instrument background, absorption, multiple scattering, and to normalize the data to absolute units using the scattering of a vanadium standard. The remaining corrections to account for the contributions from inelastic scattering by the sample, which for protons can have a pronounced dependence on the scattering vector, Q, was made using the method outlined previously[23].

Quasi-elastic Neutron Scattering Experiments

We performed QENS experiments at the National Institute of Standards and Technology (NIST) at the NIST Center for Neutron Research. The first set of experiments were taken on the Disk Chopper time-of-flight Spectrometer (DCS) using an incident wavelength of λ=7.5Å with an incident energy of E = 1.45meV resulting in a wave vector range of 0.146$Å^{-1}$ < Q < 1.574$Å^{-1}$ and an energy resolution of 35 μeV. The sample holder was composed of two concentric cylinders of aluminum of length 10cm differing by 0.1mm in diameter. The temperature range covered during this experiment for each co-solvent was (1) 263K to 298K for the glycerol co-solvent and (2) 268K to 298K for the DMSO co-solvent.

The second experiment was performed on the High Flux Backscattering Spectrometer (HFBS), using an incident wavelength of λ=6.3Å with an incident energy of E = 2.08meV, resulting

in a wave vector range of $0.6Å^{-1} < Q < 1.67Å^{-1}$ and an energy resolution of 1.0μeV. The dynamic ranges of the instrument used were adapted to the dynamics of the system +/-35μeV for high temperatures and +/-17μeV for low temperatures. This experiment was performed using two concentric cylinders of aluminum of length 4cm differing by 0.1mm in diameter. The temperature range covered during this experiment for each co-solvent was (1) 235K to 285K for the glycerol co-solvent and (2) 230K to 263K for the DMSO co-solvent.

For all sets of experiments, the data obtained were very stable during the 14 to 16 hours of collecting time. Hence, we were able to average the data to improve the data statistics and facilitate the data analysis. For all experiments the detector efficiency, energy resolution and normalization were measured using Vanadium. The spectra were corrected for contribution of the sample holder comprised of concentric aluminum cylinders. The data were corrected and analyzed using the NIST Center for Neutron Research DAVE software[24].

EXPERIMENTAL ANALYSIS

Neutron diffraction analysis

The neutron diffraction method determines the structural information in multicomponent disordered materials, and measures the elastic angular dependent scattering intensity or structure factor S(Q). The total structure factor obtained by a neutron diffraction experiment is described as:

$$S_{Tot}(Q) = \sum_{\alpha,\beta \geq \alpha} \left(2 - \delta_{\alpha\beta}\right) c_\alpha c_\beta b_\alpha b_\beta S_{\alpha\beta}(Q) \tag{1}$$

where Q is the momentum transfer, c_α corresponds to the atomic fraction and b_α represents the scattering length, and $\delta_{\alpha\beta}$ is the Kronecker delta function. The partial structure factors $S_{\alpha\beta}(Q)$ contain information about the site-site correlations $g_{\alpha\beta}(r)$ through the Fourier Transform:

$$S_{\alpha\beta}(Q) = 4\pi\rho \int_0^\infty r^2 \left[g_{\alpha\beta}(r) - 1\right] \frac{\sin Qr}{Qr} dr \tag{2}$$

where ρ is the atomic density and r is the distance between atomic centers.

To facilitate the direct extraction of the intermolecular structural correlations between water molecules and the NALMA solute in the presence of the glycerol and DMSO co-solvents at 298K, five samples were measured for each co-solvent, using the molar ratios described previously:

(1) deuterated co-solvent + d-NALMA + D_2O

(2) deuterated co-solvent +NALMA + D_2O

(3) deuterated co-solvent +50/50 d-NALMA/NALMA + D_2O

(4) deuterated co-solvent +d-NALMA + H_2O

(5) deuterated co-solvent +d-NALMA + HDO

The H/D substitution is assumed to have a negligible effect on the structure of the system studied.

The corrected data were analyzed with the Empirical Potential Structure Refinement program (EPSR)[25]. The program uses an intermolecular reference potential to represent the interactions among molecules in the simulation to initialize the model. The program is a reverse Monte Carlo method that uses the difference between the simulated and experimental diffraction data to generate a perturbation potential. When this is added to the intermolecular reference potential used to initialize the model, it operates over a series of iterations to drive the simulation into closer agreement with the experimental data. The pairwise additive reference potential used to initialize the model combines a Lennard-Jones potential with a Coulomb potential:

$$U_{\alpha\beta}(r) = 4\varepsilon_{\alpha\beta}\left[\left(\frac{\sigma_{\alpha\beta}}{r}\right)^{12} - \left(\frac{\sigma_{\alpha\beta}}{r}\right)^{6}\right] + \frac{1}{4\pi\varepsilon_0}\frac{q_\alpha q_\beta}{r} \tag{3}$$

where q_α is the atomic charge for the α atom, $\varepsilon_{\alpha\beta} = \sqrt{\varepsilon_\alpha \varepsilon_\beta}$ is the Lennard-Jones (LJ) energy scale, $\sigma_{\alpha\beta} = 0.5\left(\sigma_\alpha + \sigma_\beta\right)$ is the interparticle distance at which the energy is zero, and ε_0 is the permittivity of free space. The reference potential also maintains intra-atomic distances to define a model of the basic molecular geometry of the NALMA, water, and co-solvent molecules. We report the reference potential parameters in the Supplementary materials.

The experimental perturbation to the reference potential is defined for the i^{th} interatomic interaction as:

$$\Delta U_i(r) = FT\left[\sum_{j=1,M}\left(w_{ij}^{'}\right)^{-1}\left(S_{Tot,j}(Q) - S_{Sim,j}(Q)\right)\right] \tag{4}$$

where FT represents the Fourier transform, $w_{ij}^{'}$ combines the weight matrix and feedback factor as defined previously[26], $S_{Tot,j}$ is the j^{th} diffraction data set and $S_{Sim,j}$ is the fit obtained from the simulation. The simulations were performed using the same molar ratios used in the experiment, with the simulation box contained 20 NALMA molecules, 185 co-solvent molecules and 925 water molecules for a total of 1130 molecules for 1M NALMA in 1:5 Glycerol:H_2O for example (only the molar ratio of cosolvent to H_2O varied depending on the ratio used during the experiment). The structural configurations extracted from the Monte Carlo simulations were ensemble averaged over

5000 configurations of the simulation box.

Quasi-elastic Neutron Scattering Analysis

Quasi-elastic neutron scattering characterizes the molecular motion in liquids. Based on collection of the incoherent dynamic structure factor of water hydrogen atoms, $S_{inc}(Q,\omega)$, the QENS analysis involves fitting it to a sum of Lorentzian contributions convoluted with the instrumental resolution. We assume that $S_{inc}(Q,\omega)$ can be expressed as a convolution of three different kinds of proton motion, so that the incoherent dynamic structure factor can then be expressed as:

$$S_{inc}(Q,\omega) = e^{-\frac{1}{3}Q^2\langle u^2\rangle} S_{inc}^{trans}(Q,\omega) \otimes S_{inc}^{rot}(Q,\omega) \tag{5}$$

where the Debye-Waller factor represents the contribution from the proton vibration, $\langle u^2 \rangle$ being the mean square displacement of the proton vibration, and $S_{inc}^{trans}(Q,\omega)$ and $S_{inc}^{rot}(Q,\omega)$ are the translational and rotational dynamic structure factors.

Based on the Lorentzian fits to the scattering function, we first interpret the data using a number of analytical models traditionally applied to liquids[27-30]. The translational dynamic structure factor of diffusive motions is described by:

$$S_{trans}(Q,\omega) = \frac{1}{\pi} \frac{\Gamma_{trans}(Q)}{\omega^2 + \left(\Gamma_{trans}(Q)\right)^2} \tag{6}$$

where $\Gamma_{trans}(Q)$ is the Half Width at Half Maximum (HWHM) of a Lorentzian function[28]. When using the random jump diffusion (RJD) model, $\Gamma_{trans}(Q)$ can be interpreted as:

$$\Gamma_{trans}(Q) = \frac{D_{trans}Q^2}{1 + D_{trans}Q^2\tau_0} \tag{7}$$

where D_{trans} is the translational diffusion coefficient, and τ_0 is the residence time in one site in the liquid before jumping to another site[29]. From this model, the mean jump diffusion length, L, can be defined as:

$$L = \sqrt{6D_{trans}\tau_0} \tag{8}$$

The rotational dynamic structure factor is described by the Sears model[30] for isotropic rotational diffusion on the surface of a sphere of radius a:

$$S_{rot}(Q,\omega) = j_0^2(Qa)\delta(\omega) + \frac{1}{\pi}\sum_{l=1}^{\infty}(2l+1)j_l^2(Qa)\frac{l(l+1)D_{rot}}{\omega^2 + \left[l(l+1)D_{rot}\right]^2} \quad (9)$$

where D_{rot} is the rotational diffusion coefficient and $j_l(Qa)$ are spherical Bessel functions of order *l*. Due to the predominance of the second term for *l*=1 in Eq. (9) (for the Q range used in this study), it can be simplified to:

$$S_{inc}(Q,\omega) = e^{-\frac{1}{3}Q^2\langle u^2\rangle}\left(j_0^2(Qa)\frac{1}{\pi}\frac{\Gamma_{trans}(Q)}{\omega^2 + (\Gamma_{trans}(Q))^2} + 3j_1^2(Qa)\frac{1}{\pi}\frac{\Gamma_{rot}(Q)+\Gamma_{trans}(Q)}{\omega^2 + (\Gamma_{rot}(Q)+\Gamma_{trans}(Q))^2}\right) \quad (10)$$

where $\Gamma_{rot}(Q) = 2D_{rot}$ and the rotational time scale corresponds to: $\tau_{rot} = \frac{1}{6}D_{rot}$. We have found that analysis based on the RJD model and fits to the intermediate scattering function *I(Q,t)* give very similar translational diffusion constant estimates, and so we do not perform the latter analysis in this paper.[17, 18]

RESULTS

Liquid Diffraction Experiments

The fit of $S_{Tot}(Q)$ (Eq. (1)) compared to the experimental data for the 5 isotopic substitution runs for the 1M NALMA in 1:5 glycerol:H_2O and 1M NALMA in 1:4 DMSO:H_2O solutions are shown in Figure 2. The fitting parameter, as defined in [31], is very small for all data (ranging from 0.004 to 0.006) and visual inspection of Figure 2 ensures the accuracy of the results from the EPSR simulation. The EPSR fits to the data are in good agreement with the experimental data for Q > 1Å^{-1}, while larger residuals are observed for Q < 1Å^{-1} where the background correction and inelasticity component are difficult to assess and remove. In order to characterize any clustering of the NALMA solute molecules in water or in the presence of a given co-solvent, the intermolecular $g_{CC}(r)$ obtained from the EPSR simulation between the carbons of the NALMA molecules (labeled in Figure 1) is plotted in Figure 3a, in which we observe no clustering among solute molecules, in water or in the presence of the glycerol and DMSO co-solvents, consistent with a previous X-ray scattering study of NALMA-NALMA interactions in water.

We next determine how the hydration water interactions with the NALMA solute changes in the presence of the co-solvent. According to conventional wisdom, the DMSO co-solvent should deplete the hydration layer, while the glycerol co-solvent should be excluded from the protein

surface and therefore maintain a hydration layer[10]. We examine this effect by measuring the presence of a hydrogen bond between a water hydrogen atom and the oxygen of the carbonyl group of NALMA, as we compare $g_{HO}(r)$ in the absence or presence of either the glycerol or DMSO co-solvents (Figure 3b). The bottom curve for the 1M NALMA solution with no co-solvent clearly shows a peak at 1.8 Å with a coordination number of 1.1, which is characteristic for a hydrogen bond. Consistent with the empirical molecular rules, for these particular co-solvents at these concentrations at room temperature, the NALMA-water hydrogen bond is conserved when the kosmotropic glycerol co-solvent is added, but disappears in the presence of the DMSO co-solvent.

Another empirical distinguishing feature between chaotropes and kosmotropes is that their respective destabilizing and stabilizing effects on protein molecules correlates with their ability to disrupt water structure in the former case or to increase or maintain water structural order in the latter case[32-34]. We determine from the liquid diffraction experiments that the spatial distribution functions around the water oxygen atoms are strongly altered for the 1M NALMA in 1:4 DMSO:H_2O solution, but is largely unperturbed for the 1M NALMA in 1:5 glycerol:H_2O mixture, superficially consistent with this molecular picture. Figure 4 shows that the large second coordination shell is absent when DMSO is present, while the coordination shells when glycerol is added are very similar to the ones obtained for the NALMA peptide without any co-solvent. Therefore, we can conclude that the water layer of the NALMA solute is strongly affected by the presence of the denaturing cosolvent, which also modifies the water hydration shell.

DCS Experiments

The fits to the DCS spectra for the water dynamics measured in all NALMA/co-solvent solutions required two Lorentzians and a flat background, as did the fits to the DCS spectra for the water dynamics measured in all water/co-solvent (no NALMA) solutions. These Lorentzians were used for subsequent analysis using the RJD and Sears models to estimate the dynamical parameters D_{trans}, τ_0, and τ_{rot}. Figure 5 shows an example of the high quality of fits, including the relative residuals, for the 1M NALMA in 1:5 glycerol:H_2O and 1M NALMA in 1:4 DMSO:H_2O solutions. The narrow Lorentzian function is indicative of translational motion, while the broad Lorentzian component is identified as water rotational motion based on its lack of a Q-dependence. The background component takes into account all movements that are too fast to be observed within the chosen energy window, e.g. low energy vibrational modes. The solid line is the sum of the three fit

components. Similar quality of fits was found for all other solutions, temperatures, and Q-values.

Figure 6 shows the Full Width at High-Maximum (FWHM) of the narrow Lorentzian as a function of Q^2 for the water motions in the presence of the peptide and glycerol (Figure 6a) and DMSO (Figure 6b) co-solvents, and the best fit used in the context of the jump diffusion model is shown as a solid line over the full temperature range of the DCS experiments. The resulting diffusion coefficients, D_{trans}, and residential time, τ_0, obtained from this analysis are found in Table 1. From the Q-independence of the HWHM of the broad Lorentzian (data not shown), we derive the rotational timescale, τ_{rot}, at each temperature, which is also given in Table 1.

HFBS Experiments

The analysis of the high resolution HFBS spectrum required one Lorentzian and a background for all solutions involving the DMSO co-solvent; Figure 7a shows an example of the high quality of fits for DMSO, including the relative residuals. Similar quality of fits was found for all other DMSO solutions, temperatures, and Q-values. Notably, the single Lorentzian fit to the 1M NALMA in 1:4 DMSO:H_2O data even at low temperatures indicate only one translational motion is present, so that the effect of these DMSO denaturant is to eliminate the second water timescale observed in the original peptide-water solution.. Figure 7b shows the FWHM of the single Lorentzian as a function of Q^2, and the best fit used in the context of the jump diffusion model is shown as a solid line, for the HFBS experiment for the DMSO co-solvent. The resulting diffusion coefficients, D_{trans}, and residential time, τ_0, obtained from this analysis are found in Table 1.

The analysis of the high resolution HFBS spectrum required one Lorentzian and a background for the glycerol/water data and for the 1M NALMA in 1:5 glycerol:H_2O mixture for temperatures above 250K. However, the HFBS glycerol data for temperatures T < 250K gave a poor fit with a single Lorentzian (Figure 8a) and an additional Lorentzian is needed to obtain a good fit (Figure 8b). The additional Lorentzian for the glycerol data at low temperatures did not have a flat Q-dependence that would be consistent with rotational motion, but instead is a second water translational motion, similar to what we observed in our aqueous NALMA dynamical studies with no co-solvent at lower temperatures [17]. Figure 9 shows the FWHM of the narrow Lorentzian (Figure 9a) and the broad Lorentzian (Figure 9b) as a function of Q^2, and the best fit used in the context of the jump diffusion model is shown as a solid line, for the HFBS data for the glycerol co-solvent for temperatures T<250K. The resulting diffusion coefficients, D_{trans}, and residential time,

τ_0, obtained from the model fits to the HFBS data for glycerol are found in Table 1. It is encouraging that the overlap in temperatures for the HFBS data (265K) and the DCS data (263K) give very similar values for the translational diffusion coefficient for the 1M NALMA in 1:5 glycerol:H_2O mixture.

Arrhenius Analysis of Dynamical Parameters

Figure 10a shows the Arrhenius representation of the temperature dependence of the self-diffusion coefficient of water for the 1M NALMA in 1:4 DMSO:H_2O solution. The temperature dependence of the water dynamics for 1M NALMA with no co-solvent has been carefully characterized previously[17] where two translational motions were separated to yield a slow component showing an Arrhenius behavior and a fast component with a non-Arrhenius temperature dependence. However, we find that in the presence of the chaotropic DMSO co-solvent, the water dynamics only shows a single translational motion with an Arrhenius dependence on temperature, with an activation energy of 6.9 kcal/mole. As a reference state we also show the pure DMSO/water co-solvent mixture (i.e. without the NALMA solute) in which we see that the water dynamics is somewhat faster, but it exhibits virtually the same temperature dependence and activation energy of 6.6 kcal/mole compared to that with the peptide present.

In Figure 10b we plot the mean jump length $L = (6D_{trans}\tau_0)^{1/2}$, obtained from the jump diffusion analysis of the translational hydration water data for the DMSO solutions with and without the NALMA peptide over the DCS and HFBS experiments with temperature. The mean jump length obtained for the water in 1M NALMA without co-solvent shows a confinement signature for the slow component of the water dynamics with a positive slope[17] as observed previously observed for water at the surface of proteins[35]. This confinement signature is not observed in the presence of the denaturant DMSO solvent, and the temperature dependence of the mean jump length is similar to the temperature dependence of bulk water. These dynamical results are consistent with the loss of hydrogen-bonding of water to the peptide in the presence of the denaturing DMSO solvent as seen in the diffraction data, and because water is displaced from the peptide surface, its influence is negated in the temperature dependence of the water dynamics. In fact the chaotropic co-solvent dictates the Arrhenius dependence of the water dynamics.

For the 1M NALMA in 1:5 d-Glycerol:H_2O solution, we have reanalyzed the DCS/HFBS dynamics at higher temperatures with the assumption of two translational components as we did in

our original NALMA study, since two Lorentzians are required to fit the low temperature HFBS data. We do this by assuming that the slower translational component at lower temperatures continues to follow an Arrhenius dependence when extrapolated to temperatures above 255K. This allows us to fix this translational motion as a known quantity to estimate the diffusion constant for the second translational process for temperatures of 263-298K. Figure 11a presents the Arrhenius representation of the diffusion coefficient D_{trans} corresponding to the combination of the DCS and HFBS data treatment for the 1M NALMA in 1:5 d-Glycerol:H_2O solution. Overall the kosmotropic co-solvent perturbs the quantitative values of the self-diffusion constants of the original 1M NALMA system, but since it does not disturb the hydration layer near the peptide, all of the anomalous water dynamics are preserved including the two translational motions and their dependence with temperature.

In Figure 11b we plot the mean jump length $L = (6D_{trans}\tau_0)^{1/2}$, obtained from the jump diffusion analysis of the translational hydration water data for the NALMA-glycerol and water solution. We see a strong separation in residence times for the two diffusional timescales (Table 1) that manifests itself in exhibiting qualitatively different trends in the mean jump length with temperature. The faster diffusional timescale shows an increasing mean jump length as temperature is lowered, and thus the same negative slope that has been observed in bulk supercooled water[33], while the slower diffusional timescale shows the opposite slope, similar to the behavior observed for supercooled water interacting with vycor[33] or protein surfaces[34]. Thus the two translational timescales we measure show trends in mean jump length in which the slow component is due to confinement and the bound water at the NALMA surface, while the faster diffusional timescale is due to translational motions of outer hydration layers that are similar to bulk supercooled water.

DISCUSSION AND CONCLUSION

There continues to be debate in regards the mechanism of protein stabilization or destabilization by co-solvents [32], although that debate is often focused more directly on the Hofmeister series of ionic additives [36], as opposed to the non-ionic co-solvents investigated here. An indirect mechanism proposes that chaotropes disrupt water structure so as to enhance solubilization of hydrophobic groups, thus shifting the equilibrium to the unfolded state, whereas kosmotropes increase water structure so as to diminish the solubilization of hydrophobic groups, thus stabilizing the folded state. A number of studies have sought to determine structural changes,

or thermodynamic consequences of structural changes in water with co-solvents with mixed results [32, 33, 36-38], suggesting that the indirect mechanism is a poor predictor of co-solvent behavior on protein stabilization. A more direct mechanism proposes that chaotropes or denaturants preferentially bind to the protein, thereby dehydrating the protein surface to promote the unfolded state, while stabilizing kosmotropic agents do not interact with the biological macromolecule, leading to a preferential hydration of the protein surface that favors the folded state.

We have determined that aspects of both mechanisms are true in the case of the DMSO co-solvent examined here. First the direct mechanism is supported by the observation that the hydration layer of the NALMA solute is largely destroyed by the denaturant at high concentrations of both DMSO and peptide. We show in a companion paper that the DMSO solvent displaces the water near the hydrophobic regions of NALMA due to direct favorable hydrophobic interactions of the denaturant with the peptide itself. [39] At the same time, DMSO replaces water in its own hydration shell, and the water dynamical trends with temperature are completely determined by the DMSO co-solvent regardless of the presence or absence of peptide. The two translational timescales of the original peptide water system, one of which is non-Arrhenius, collapses to a single translational process that exhibits an Arrhenius temperature dependence. This is consistent with previous studies using neutron diffraction, QENS and molecular dynamics simulation on DMSO/water co-solvent mixtures without the peptide solute.[40-42] Those studies showed that the self-diffusion coefficient of water exhibited an Arrhenius temperature dependence, unlike the non-Arrhenius behavior that is observed for pure water bulk solvent. Furthermore, it was shown while the water dynamics is strongly affected by the concentration of DMSO, the DMSO dynamics is only weakly perturbed by the molar ratio of the two co-solvents, consistent with the longer hydrogen bond lifetimes between DMSO and water as compared to that between water molecules. We would refine the language of structure breaking in this case to be a co-solvent additive that supercedes the usual structural and dynamical signatures of the water solvent.

By contrast, we have found that water has stable hydrogen-bonded interactions with the amphiphilic peptide in the presence of glycerol, exactly the same structural signature as protein systems studied by QENS[43], fluorescence spectroscopy[44], and densimetric method[45] which shows that the protein competes favorably with glycerol for water molecules. The maintenance of this hydration layer in turn allows for a clear separation of translational timescales for the hydration layer from the more bulk-like water population, consistent with the original hydration dynamical

signatures observed for the aqueous peptide system without the glycerol co-solvent. In this case, the direct mechanism is supported, whereby the kosmotropic co-solvent is clearly more excluded from the protein surface to yield a "preferential" hydration layer. In this case structural effects on water appear to be negligible, casting doubt on the usefulness of the indirect mechanism as a fully encompassing predictor of co-solvent behavior.

ACKNOWLEDGMENTS. We gratefully acknowledge the support of the Department of Energy, Condensed Phase and Interfacial Molecular Science Program, DE-AC02-05CH11231. We are grateful to J.R.D. Copley, Craig Brown, and Timothy Jenkins for generous support and discussion. This work utilized facilities supported in part by the National Science Foundation under Agreement No. DMR-0086210. We acknowledge the support of the National Institute of Standards and Technology, U.S. Department of Commerce, in providing the neutron research facilities used in this work. Certain commercial materials are identified in this paper to foster understanding. Such identification does not imply recommendation or endorsement by the National Institute of Standards and Technology, nor does it imply that the materials or equipment identified are necessarily the best available for the purpose.

REFERENCES

[1] L. N. Bell*, Biotechnology Progress*, 1997, **13**, 342-346.

[2]M. Buck, *Quarterly Reviews of Biophysics*, 1998, **31**, 297-355.

[3] Z. Ignatova and L. M. Gierasch, *Methods Enzymol.*, 2007, **428**, 355-372.

[4] N. K. Jain and I. Roy, *Protein Science*, 2009, **18**, 24-36.

[5] C. N. Pace, *Methods Enzymol.*, 1986, **131**, 266-280.

[6] G. I. Makhatadze, *J. Phys. Chem. B*, 1999, **103**, 4781-4785.

[7] L. Ramirez-Silva, J. Oria-Hernandez, S. Uribe, in *Encyclopedia of Surface And Colloid Science*; ed. P. Somasundaran, (Taylor & Francis, 2006).

[8] M. G. Cacace, E. M. Landau, J. J. Ramsden, *Q. Rev. Biophys.*, 1997, **30**, 241−278.

[9] S. N. Timasheff, in *Water and Life*, ed. G.S. Somero (Springer Verlag, Berlin, 1992) p. 70.

[10] S. N. Timasheff, *Proc. Natl. Acad. Sci. USA,* 2002, **99**, 9721-9726.

[11] P. M. Wiggins, *Cell. Mol. Biol.,* 2001, **47**, 735-744.

[12] S. N. Timasheff, *Ann. Rev. Biophys. Biomol. Struc.*, 1993, **22**, 67-97.

[13] D. Russo, R. K. Murarka, G. Hura, E. R. Verschell, J. R.D. Copley, and T. Head-Gordon, *J. Phys. Chem. B*, 2004, **108**, 19885-19893.

[14] D. Russo, G. Hura, and T. Head-Gordon, *Biophys. J.,* 2004*,* **86**, 1852-1862.

[15] D. Russo, R. K. Murakra, J. R.D. Copley, and T. Head-Gordon, *J. Phys. Chem. B* 2005, **109**, 12966-12975.

[16] R. K. Murakra and T. Head-Gordon, *J. Chem. Phys.,* 2007, **126**, 215101-215109.

[17] C. Malardier-Jugroot and T. Head-Gordon, *Phys. Chem. Chem. Phys.*, 2007, **9**, 1962-1971.

[18] C. Malardier-Jugroot, M. E. Johnson, R. K. Murarka, and T. Head-Gordon, *Phys. Chem. Chem. Phys.*, 2008, **10**, 4903-.

[19] M.E. Johnson, C. Malardier-Jugroot, R.K. Murarka, and T. Head-Gordon, *J. Phys. Chem. B* 2008, **113**, 4082–4092.

[20] R. K. Murakra and T. Head-Gordon, *J. Phys. Chem. B,* 2008, **112**, 179-186.

[21] CDN Isotopes (Pointe-Claire, Canada).

[22] A. K. Soper, W. S. Howells, and A. C. Hannon, Report No. RAL-89-046, 1989.

[23] A. K. Soper and A. Luzar, *J. Chem. Phys.*, 1992, **97**, 1320-.

[24] http://www.ncnr.nist.gov/dave

[25] A. K. Soper, *Mol. Phys.*, 2001, **99**, 1503-1516.

[26] A. K. Soper, *Phys. Rev. B*, 2005, **72**, 104204

[27] M. Bee, *Quasi-elastic neutron scattering*, Adam Hilger, Philadelphia, 1988.

[28] M. Bee, *J. de Physique IV*, 2000, **10**, 1-14.

[29] M. Bee, *Chem. Phys.*, 2003, **292**, 121-141.

[30] V. F. Sears, *Can. J. Phys.*, 1966, **44**, 1299-.

[31] A.K. Soper, *Chemical Physics*, 1996, **202** , 295-306

[32] Y. Marcus, *Chem. Rev.*, 2009, **109**, 1346-1370.

[33] J. D. Batchelor, A. Olteanu, A. Tripathy and G. J. Pielak, *J. Am. Chem. Soc.*, 2004, **126**, 1958-1961.

[35] J. Teixeira, M.-C. Bellissent-Funel, S. H. Chen, and A. J. Dianoux*, Phys. Rev. A,* 1985, **31**, 1913-.

[35] J.-M. Zanotti, M.-C. Bellissent-Funel and S. H. Chen,, *Phy. Rev. E*, 1999, **59**, 3-**.**

[36] Y. Zhang and P. S. Cremer, *Curr. Opin. Chem. Bio.*, 2006, **10**, 658-663.

[37] A. W. Omta, M. F. Kropman, S. Woutersen and H. J. Bakker, *Science*, 2003, **301**, 347–349.

[38] F. Vanzi, B. Madan, and K. Sharp, *J. Am. Chem. Soc.*, 1998, 120, 10748-10753.

[39] M. E. Johnson, C. Malardier-Jugroot, and T. Head-Gordon, *in preparation,* 2009.

[40] A. Luzar and D. Chandler, *J. Chem. Phys.*, 1993, **98**, 8160-.

[41] I. A. Borin and M. S. Skaf, *J. Phys. Chem.*, 1999, **110**, 6412-.

[42] J. Cabral, A. Luzar, J. Teixeira and M-C. Bellissent-Funel, *J. Chem. Phys.*, 2000, **113**, 19-.

[43] A. Paciaroni, A. Orecchini, S. Cinelli, G. Onori, R.E. Lechner and J. Pieper, *Chem. Phys.,* 2003, **292**, 397-.

[44] G. S. Lakshmikanth and G. Krishnamoorthy, *Biophys. J.*, 1999, **77**, 1100-.

[45] K. Gekko and S. N. Timasheff, *Biochem.*, 1981, **20**, 4667-.

Table 1: *Translational diffusion coefficient D_{trans}, residential time τ_0, and τ_{rot} of water in the peptide solutions with co-solvents glycerol and DMSO.* The analysis of the DCS and HFBS (in bold) data using the random jump diffusion model yielded the same translational diffusion constants when temperatures overlapped.

1M NALMA in 1:5 Glycerol:H_2O							
Temperature (K)	**300**	**288/285**	**277**	**263/265**	**255**	**245**	**235**
D_{trans} (10^{-5} cm^2/s) DCS/HFBS	0.43	0.32	0.21	0.12	**0.156**	**0.117**	**0.069**
D_{trans}($10^{-5}cm^2/s$) HFBS		**0.28**		**0.13**	**0.027**	**0.015**	**0.006**
τ_0 (ps) DCS	10.8	15.0/31.9	18.5	25.2/84.3	20.6	33.6	86.7
τ_0 (ps) HFBS					98	190	400
τ_{rot} (ps) DCS	2.55	2.73	2.96	3.18			
1:5 Glycerol:H_2O							
Temperature (K)	**298**	**288**	**277**	**263/265**	**255**	**245**	**235**
D_{trans} (10^{-5} cm^2/s) DCS/HFBS	0.526	0.382	0.240	0.125			
D_{trans}($10^{-5}cm^2/s$) HFBS				**0.127**	**0.076**	**0.041**	**0.020**
τ_0 (ps) DCS/HFBS	6.98	10.1	13.5	25.1/41.4	76.9	208	401
τ_{rot} (ps) DCS	2.32	2.59	3.51	3.75			
1M NALMA in 1:4 DMSO:H_2O							
Temperature (K)	**298**	**288**	**277**	**268**	**263**	**248**	**230**
D_{trans} (10^{-5} cm^2/s) DCS/HFBS	0.55	0.38	0.24	0.18	**0.11**	**-**	**0.017**
τ_0 (ps) DCS/HFBS	3.46	4.15	6.14	8.59	**20**	**-**	**384**
τ_{rot} (ps) DCS	2.04	2.31	2.82	2.99			
1:4 DMSO:H_2O							
Temperature (K)	**298**	**288**	**277**	**271**	**263**	**248**	**230**
D_{trans} (10^{-5} cm^2/s) DCS/HFBS	0.75	0.54	0.37	0.25	**0.18**	**0.084**	**0.0304**
τ_0 (ps) DCS/HFBS	3.21	4.21	6.11	7.08	**11**	**37**	**176**
τ_{rot} (ps) DCS	2.05	2.27	2.42	2.71			

FIGURE CAPTIONS

Figure 1: *The chemical structure of n-acetyl-leucine-methylamide (NALMA), the peptide solute used in this study.*

Figure 2: *Experimentally measured total structure factor F(Q) (symbols) and EPSR refined fits (solid lines) for neutron scattering data collected on* (a) 1M NALMA without any co-solvent, (b) 1M NALMA in 1:5 glycerol:H_2O, (c) 1M NALMA in 1:4 DMSO:H_2O. Each curve is a different isotopic content in order from top to bottom: the completely deuterated solution, d-NALMA in HDO, d-NALMA in H_2O, 50/50 d-NALMA/NALMA in D_2O, NALMA in D_2O (the added co-solvent is always deuterated).

Figure 3: *Site−site radial distribution functions derived by the EPSR calculations.* (a) $g_{CC}(r)$ of the intermolecular NALMA methyl carbons (continuous lines) together with the coordination number $n_{CC}(r)$ (dotted lines). No clustering of the NALMA molecules is observed with or without co-solvents. (b) $g_{HO}(r)$ of the water hydrogen atom around the oxygen of the carbonyl group of NALMA (continuous lines) together with the coordination number n(r) (dotted lines). The coordination number for the hydrogen bond integrated to 3.1Å is 1.1 for 1M NALMA and 1.0 for 1M NALMA and glycerol, but is close to zero for DMSO and thiocyanate. In order from top to bottom: 1M NALMA without co-solvent, 1M NALMA in 1:5 glycerol:H_2O, 1M NALMA in 1:4 DMSO:H_2O.

Figure 4: *Spatial distribution functions of the water oxygen atoms around a central water molecule, with an fractional isosurface level of 0.15 and a minimum and maximum radius of plotof 2.0 and 6.5Å respectively.* (a) 1M NALMA without co-solvent, (b) 1M NALMA in 1:5 glycerol:H_2O, and (c) 1M NALMA in 1:4 DMSO:H_2O. The density was plotted in the range 2.0–6.5 Å (the first and second coordination shells) for the water-NALMA solution.

Figure 5: *Incoherent structure factor DCS spectrum of water*. (a) 1M NALMA in 1:5 glycerol:H_2O at 288K and Q=0.85 $Å^{-1}$ and (b) 1M NALMA in 1:4 DMSO:H_2O at 288K and Q=0.95$Å^{-1}$. The upper curve shows the experimental curve as circles, the total fit component as a continuous line, and the two Lorentzian and background components as dashed lines. The lower curve shows the typical residual obtained from the fit.

Figure 6: *Full width at half-maximum as a function of Q^2 for water dynamics as a function of temperature for the DCS experiment (symbols).* (a) 1M NALMA in 1:5 glycerol:H_2O and (b) 1M NALMA in 1:4 DMSO:H_2O. The translational motion was fit to a Lorentzian used in the jump diffusion model (fit represented by the continuous lines).

Figure 7: *(a) Incoherent structure factor HFBS spectrum for water at Q=0.87 $Å^{-1}$ for 1M NALMA in 1:4 DMSO:H_2O at 230K.* The upper curve shows the experimental curve as circles, the total fit component as a continuous line, and the single Lorentzian and background components as dashed lines. The lower curve shows the typical residual obtained from the fit. *(b) Full width at half-maximum as a function of Q^2 for water dynamics as a function of temperature for the HFBS experiment (symbols) for 1M NALMA in 1:4 DMSO:H_2O.* The translational motion was fit to a Lorentzian used in the jump diffusion model (fit represented by the continuous lines).

Figure 8: *Incoherent structure factor HFBS spectrum for water at $Q=0.75Å^{-1}$ for 1M NALMA in 1:5 glycerol:H_2O at 245K.* The fits use a flat background and (a) a single Lorentzian or (b) two Lorentzian functions. The upper curve shows the experimental curve as circles, the total fit component as a continuous line, and the single or double Lorentzian and background components as dashed lines. The lower curve shows the typical residual obtained from the fit.

Figure 9: *Full width at half-maximum as a function of Q^2 for water as a function of temperature obtained for the HFBS experiments (symbols*). (a) narrow Lorentzian and (b) broader Lorentzian. The translational motion was fit to a Lorentzian used in the jump diffusion model (fit represented by the continuous lines).

Figure 10: *(a) Arrhenius representation of the experimentally determined D_{trans} for water in the presence of peptide and DMSO co-solvent.* We also display the two translational diffusive motions for the water dynamics for aqueous NALMA without co-solvent; slow component (open squares) and fast component (crossed squares) for temperatures between 248K and 288K. *(b) Temperature dependence of the mean jump length of water dynamics water in the presence of peptide and DMSO co-solvent.* We also show the mean jump length for the water dynamics for aqueous NALMA without co-solvent; slow component (open squares) and fast component (crossed squares) for temperatures between 248K and 288K.

Figure 11: *(a) Arrhenius representation of the experimentally determined D_{trans} for water in the presence of peptide and glycerol co-solvent.* We also display the two translational diffusive motions for the water dynamics for aqueous NALMA without co-solvent; slow component (open squares) and fast component (crossed squares) for temperatures between 248K and 288K. *(b) Temperature dependence of the mean jump length of water dynamics water in the presence of peptide and glycerol co-solvent.* We also show the mean jump length for the water dynamics for aqueous NALMA without co-solvent; slow component (open squares) and fast component (crossed squares) for temperatures between 248K and 288K.

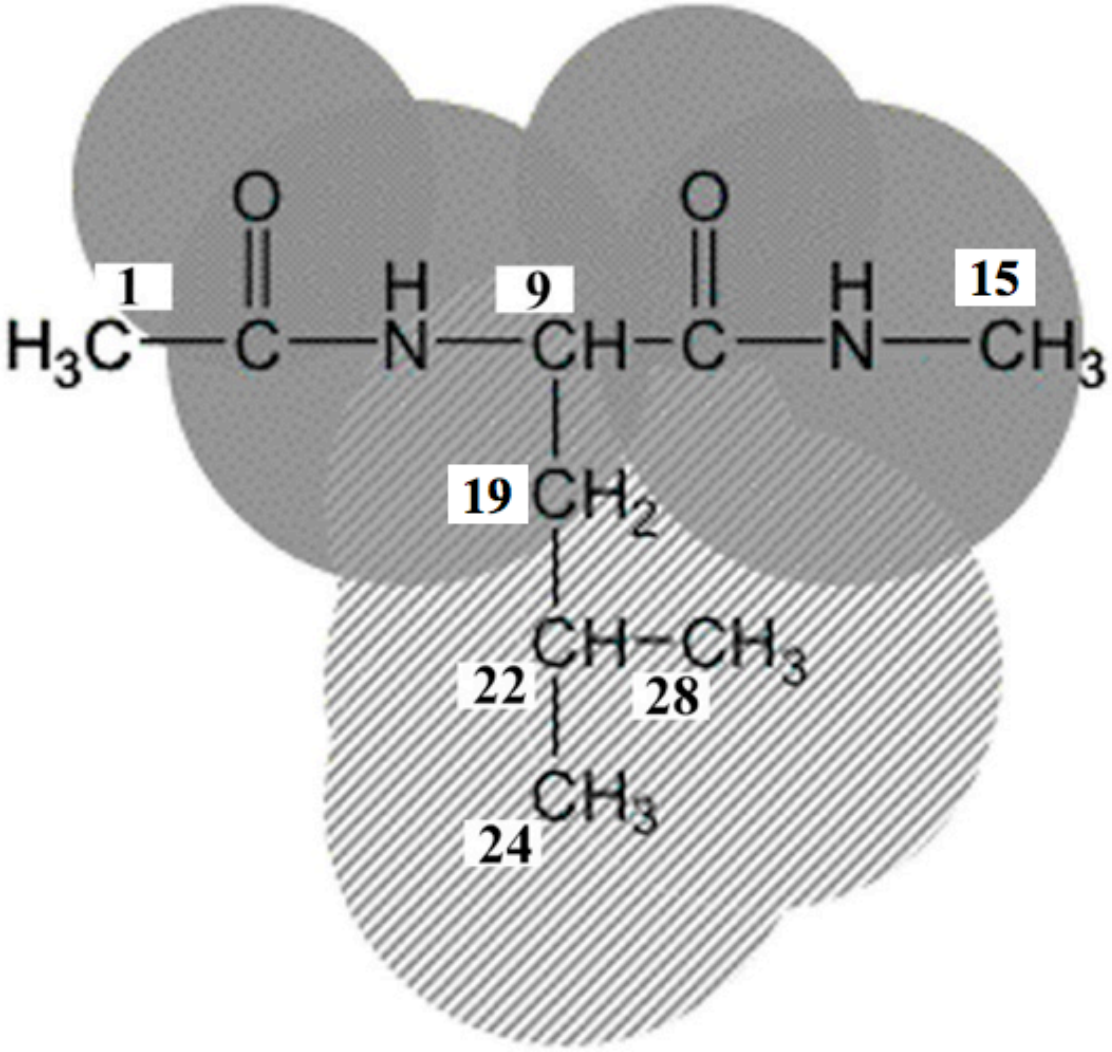

Figure 1. Malardier-Jugroot et al

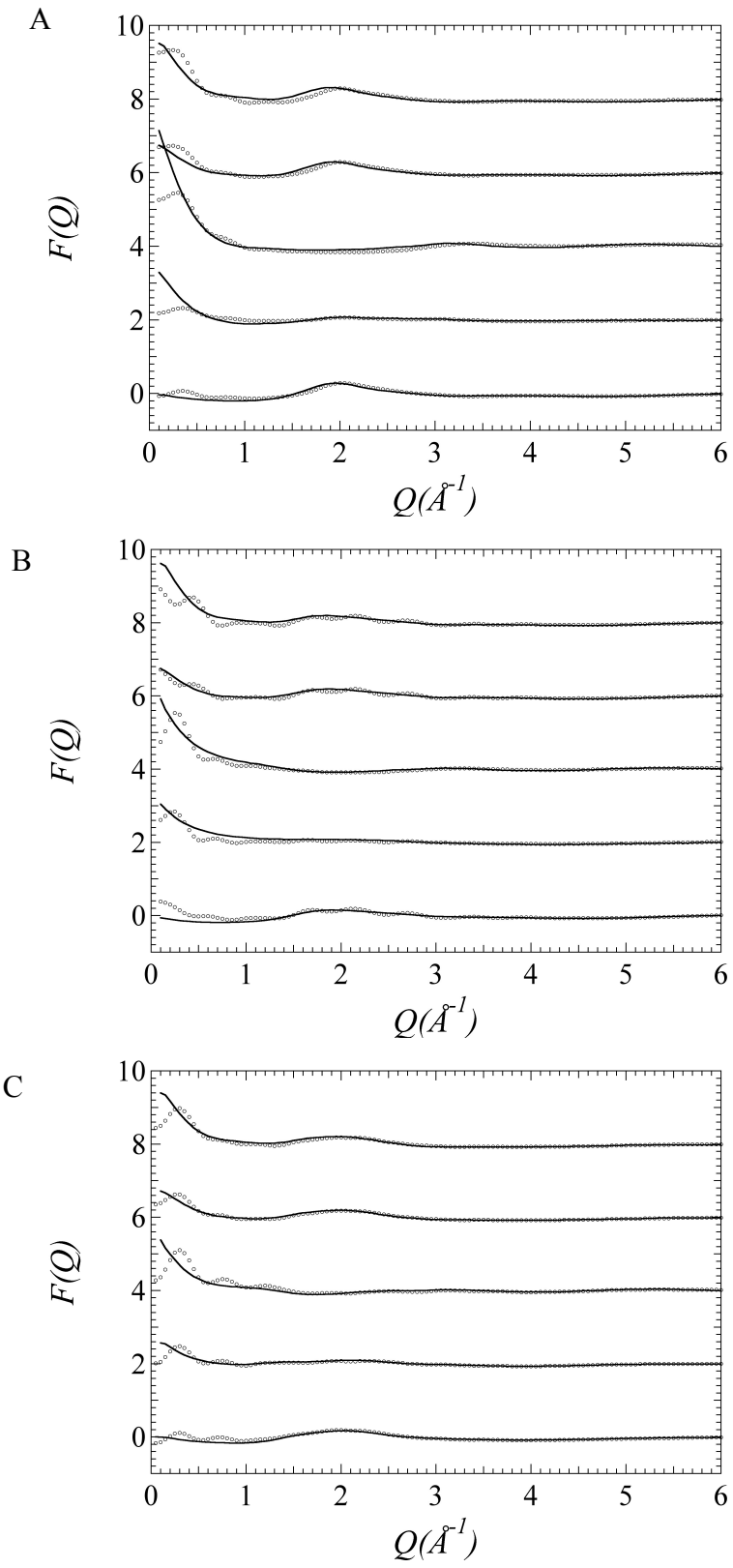

Figure 2. Malardier-Jugroot et al

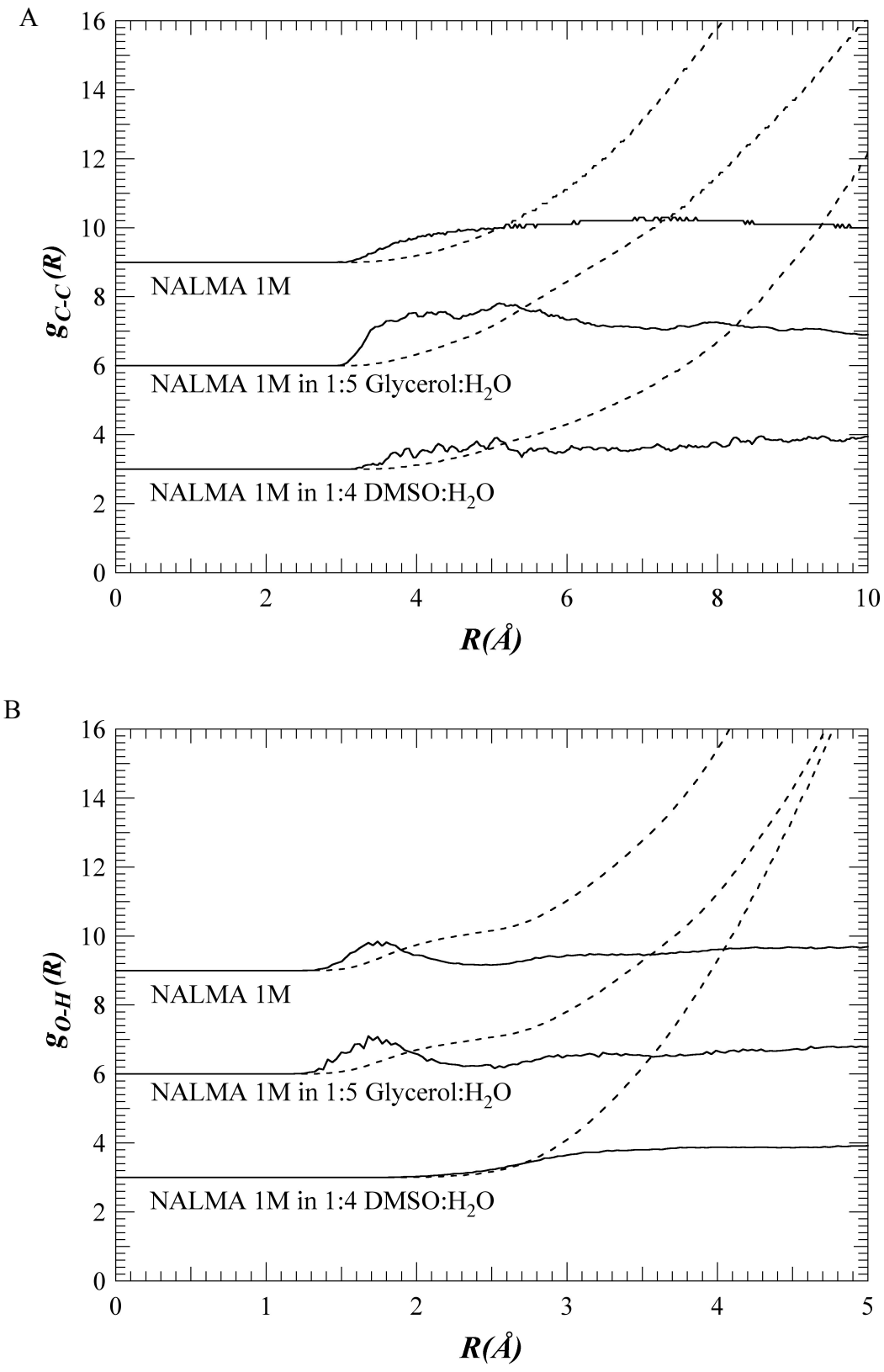

Figure 3. Malardier-Jugroot et al

A

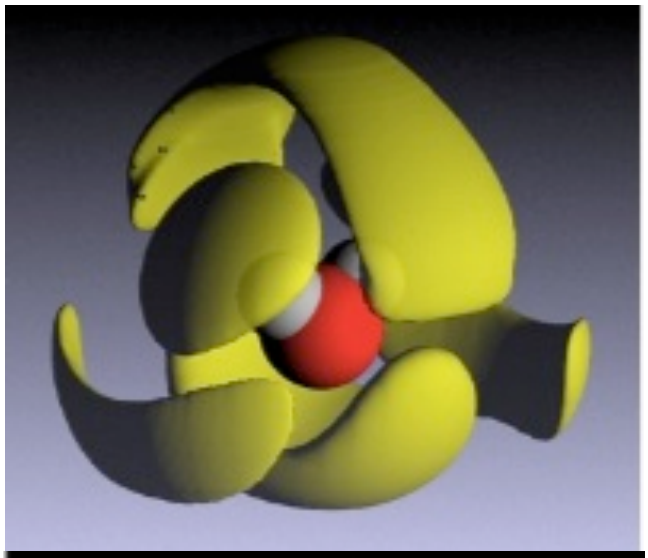

B

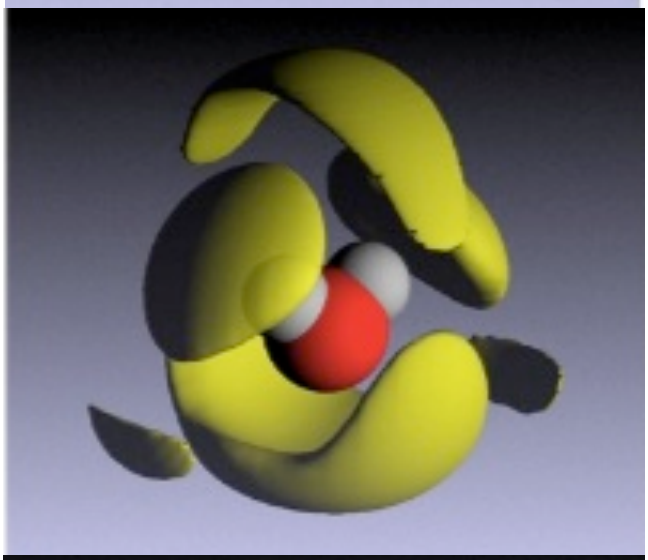

C

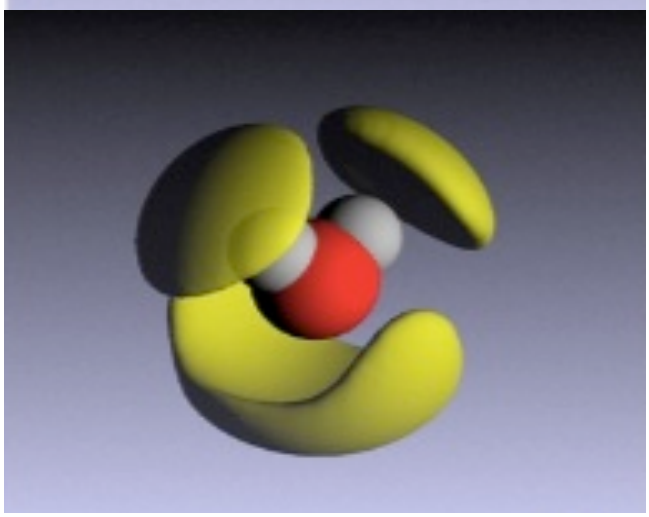

Figure 4. Malardier-Jugroot et al

A

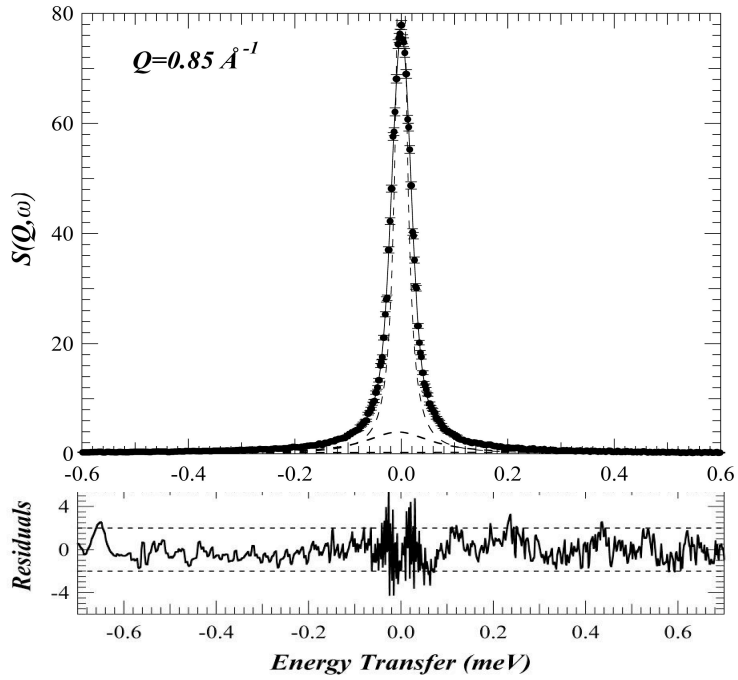

B

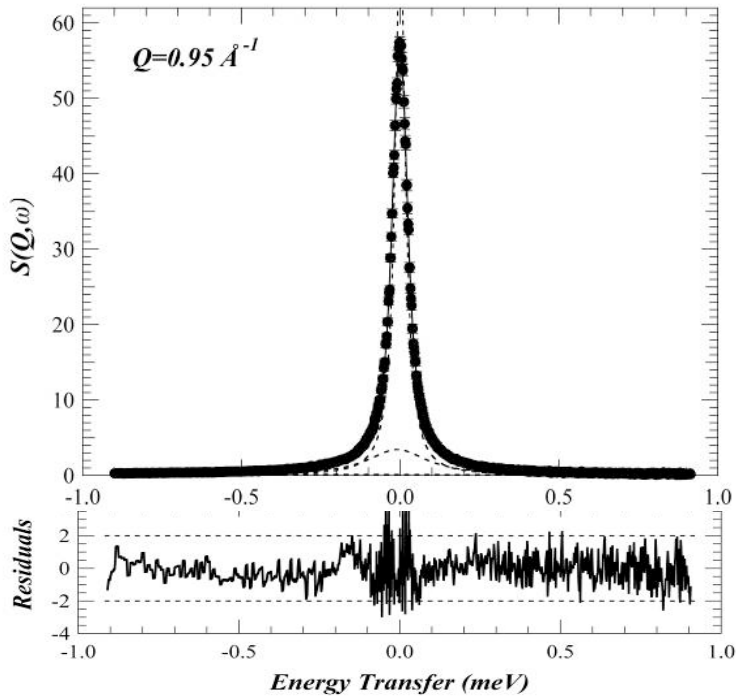

Figure 5. Malardier-Jugroot et al

A

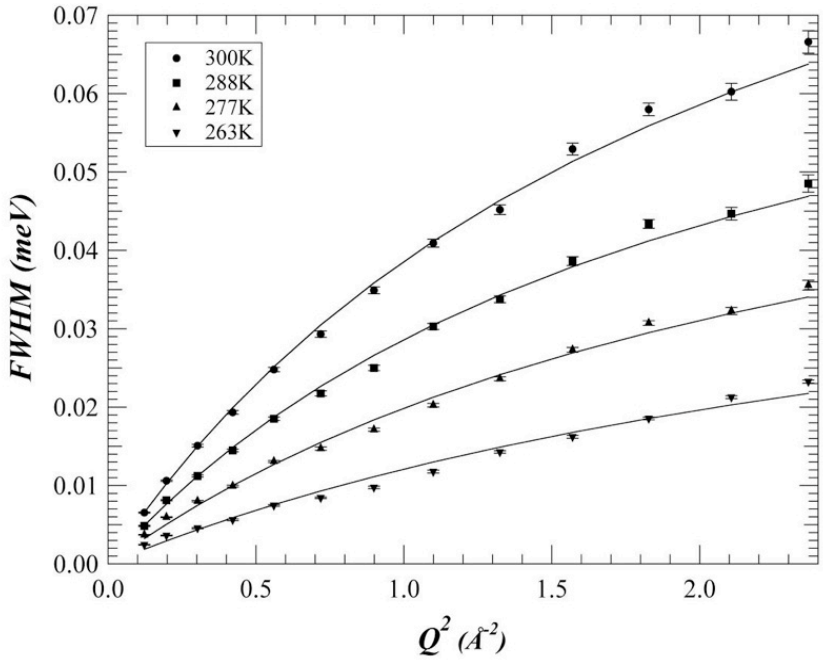

B

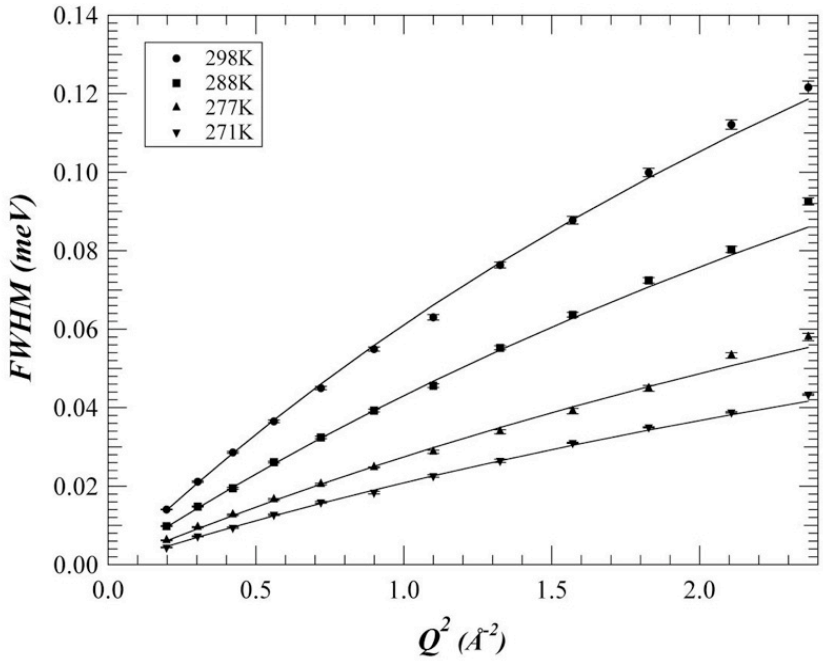

Figure 6. Malardier-Jugroot et al

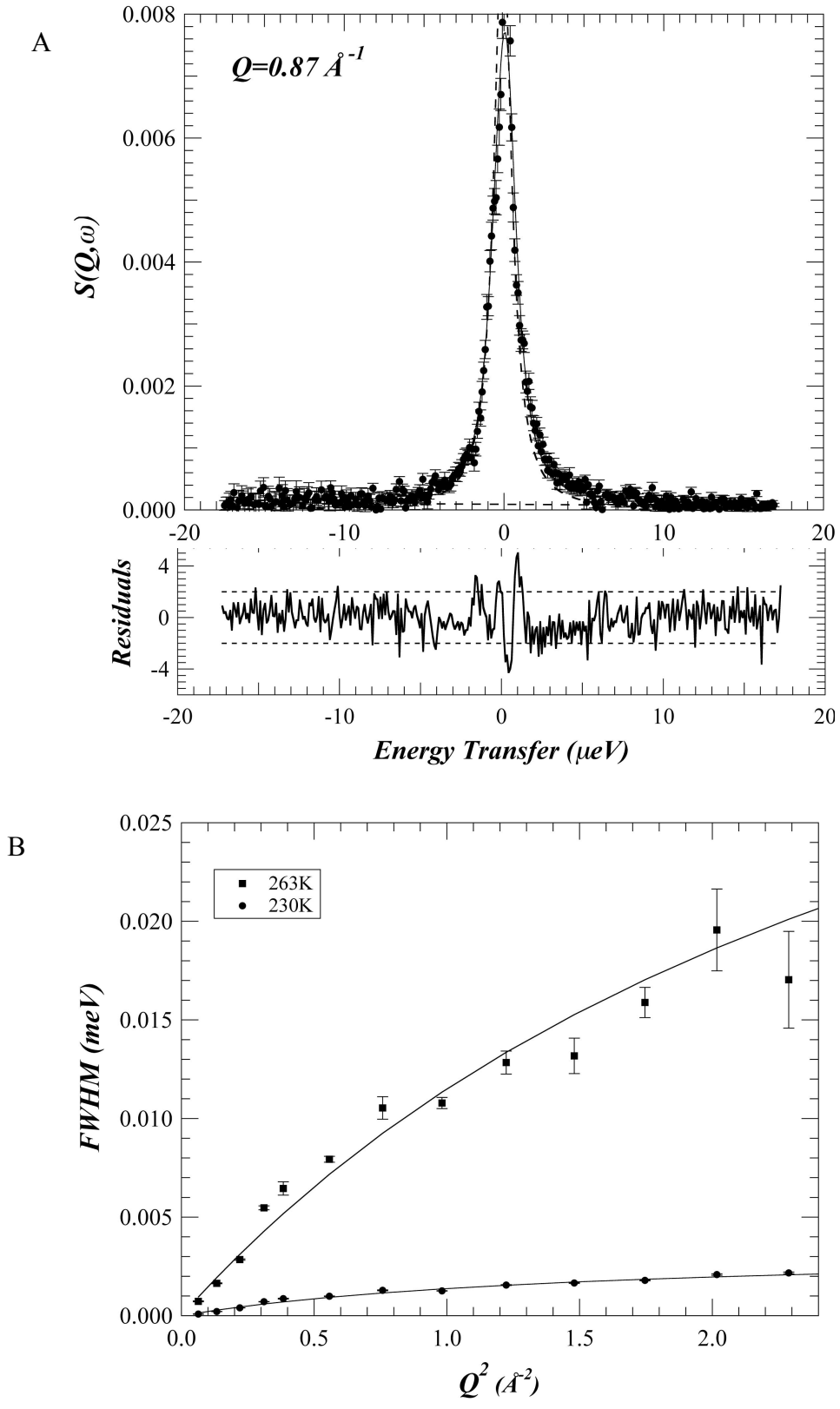

Figure 7. Malardier-Jugroot et al

A

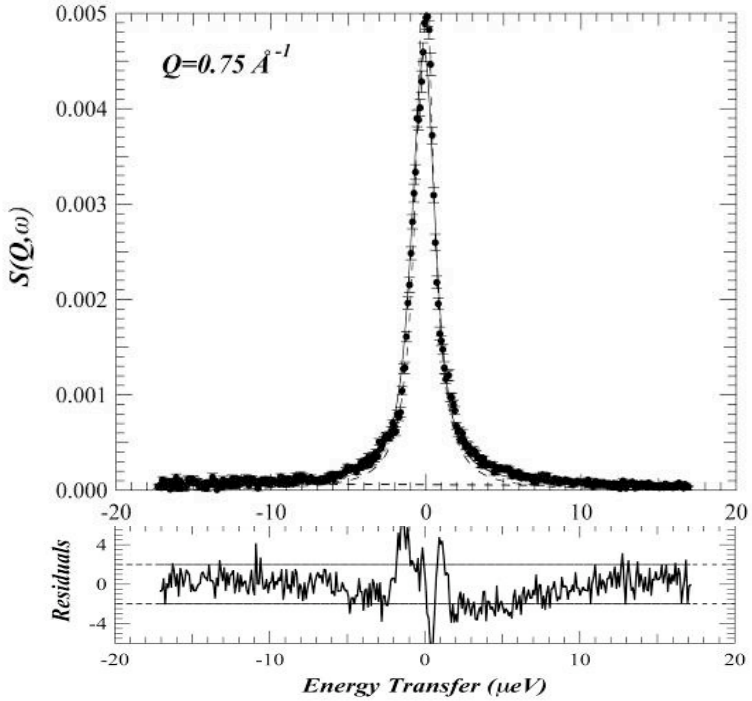

B

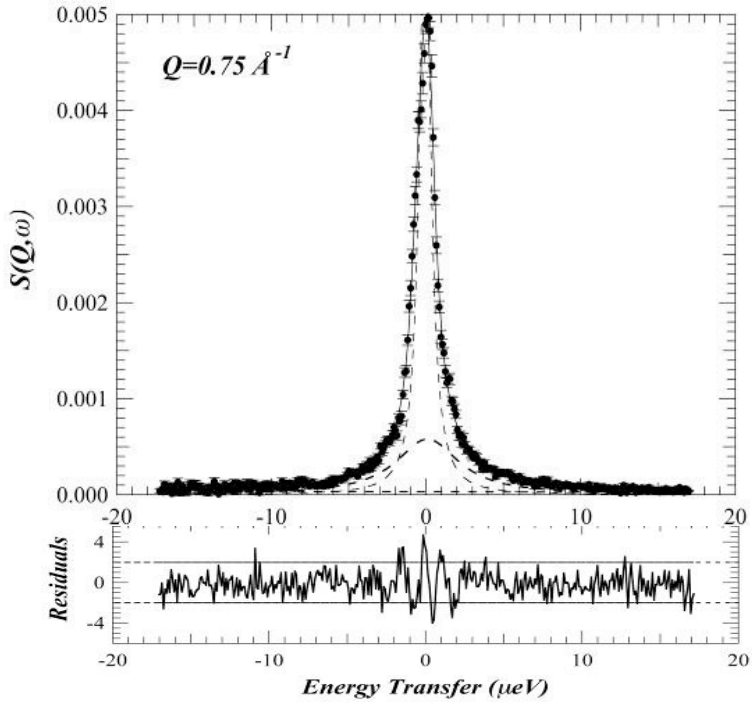

Figure 8. Malardier-Jugroot et al

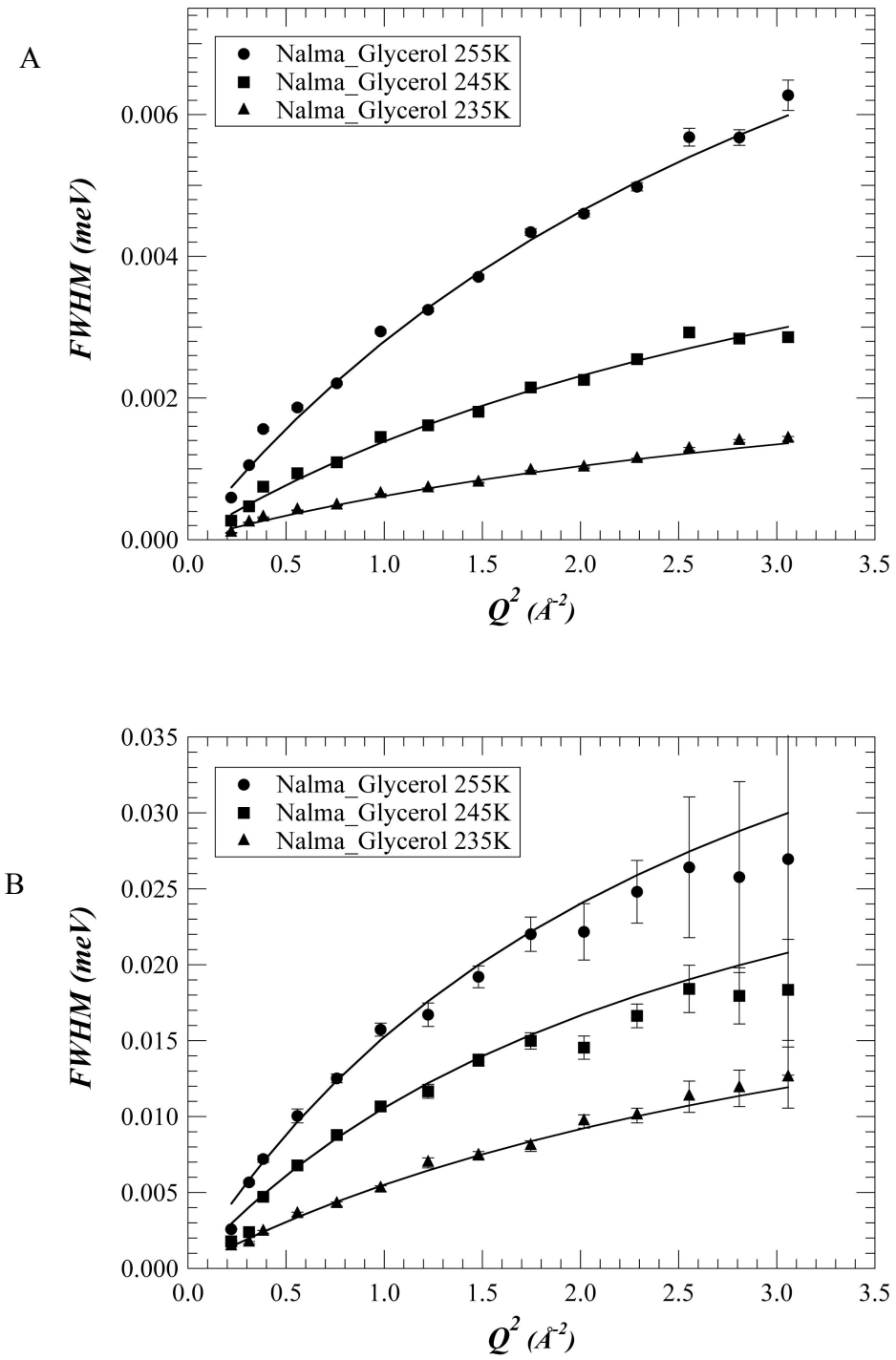

Figure 9. Malardier-Jugroot et al

A

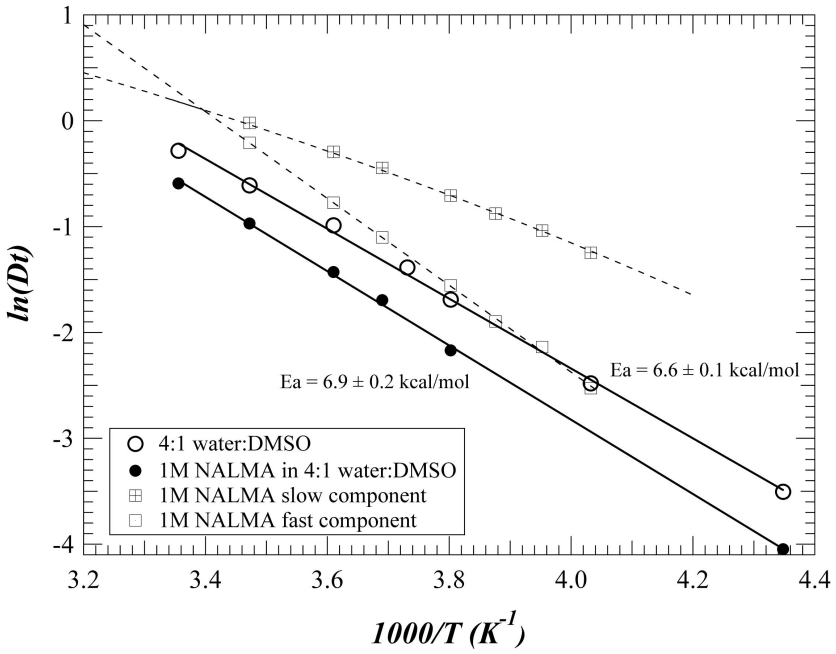

B

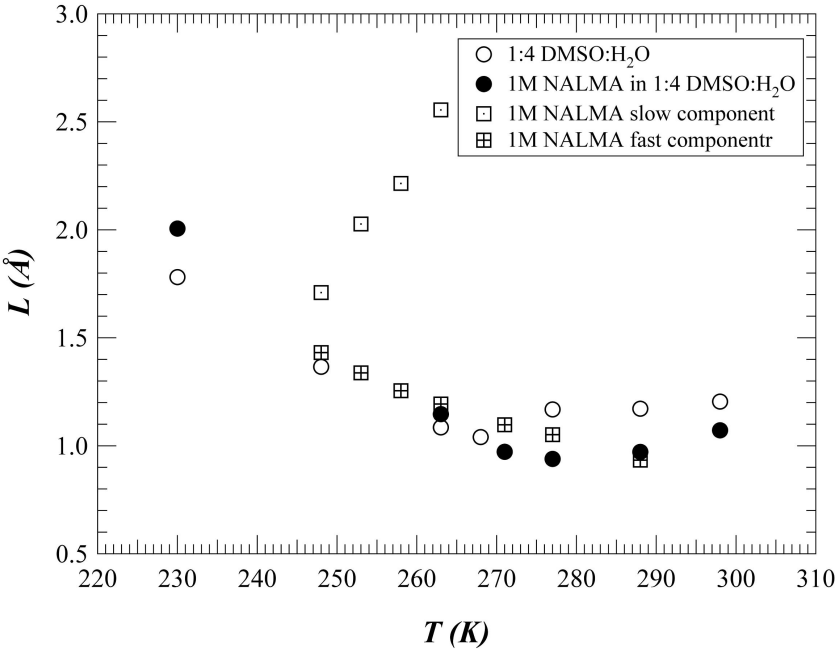

Figure 10. Malardier-Jugroot et al

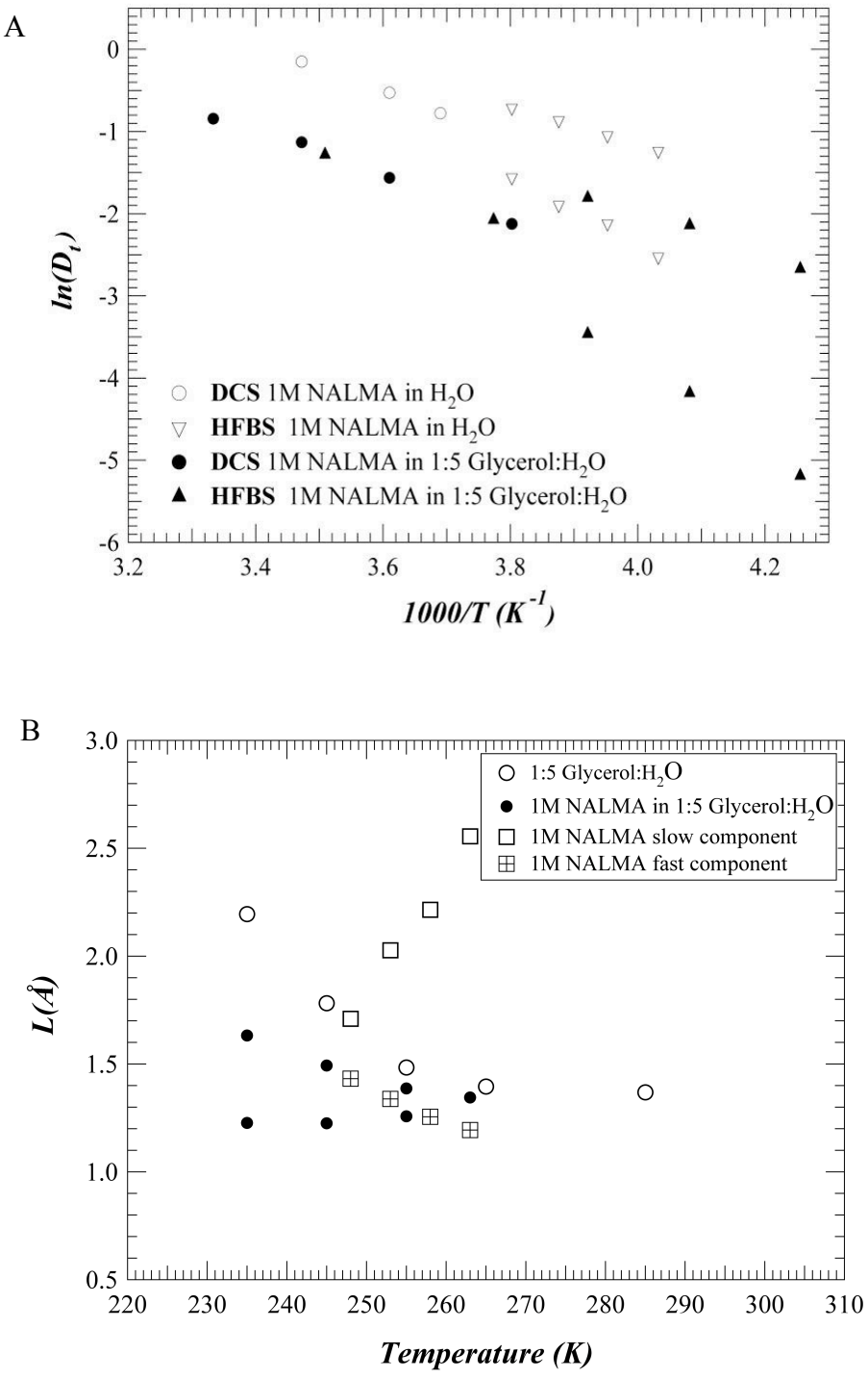

Figure 11. Malardier-Jugroot et al